The EMBO Journal (2010) 29, 1318–1330 | © 2010 European Molecular Biology Organization | All Rights Reserved 0261-4189/10
www.embojournal.org

THE EMBO JOURNAL

AP-1/σ1B-adaptin mediates endosomal synaptic vesicle recycling, learning and memory

Nataliya Glyvuk[1,2,6], Yaroslav Tsytsyura[1,2,6], Constanze Geumann[3,5,6], Rudi D'Hooge[4], Jana Hüve[2], Manuel Kratzke[3], Jennifer Baltes[3], Daniel Böning[1,2], Jürgen Klingauf[1,2,*] and Peter Schu[3,*]

[1]Institute of Medical Physics and Biophysics, University of Münster, Münster, Germany, [2]Max-Planck Institute for Biophysical Chemistry, Department of Membrane Biophysics, Göttingen, Germany, [3]Biochemistry II, Georg-August University, Göttingen, Germany and [4]Laboratory of Biological Psychology, University of Leuven, Leuven, Belgium

Synaptic vesicle recycling involves AP-2/clathrin-mediated endocytosis, but it is not known whether the endosomal pathway is also required. Mice deficient in the tissue-specific AP-1–σ1B complex have impaired synaptic vesicle recycling in hippocampal synapses. The ubiquitously expressed AP-1–σ1A complex mediates protein sorting between the *trans*-Golgi network and early endosomes. Vertebrates express three σ1 subunit isoforms: A, B and C. The expressions of σ1A and σ1B are highest in the brain. Synaptic vesicle reformation in cultured neurons from σ1B-deficient mice is reduced upon stimulation, and large endosomal intermediates accumulate. The σ1B-deficient mice have reduced motor coordination and severely impaired long-term spatial memory. These data reveal a molecular mechanism for a severe human X-chromosome-linked mental retardation.

The EMBO Journal (2010) **29,** 1318–1330. doi:10.1038/emboj.2010.15; Published online 4 March 2010
Subject Categories: membranes & transport; neuroscience
Keywords: adaptor protein complex; clathrin; sigma1; synaptic vesicles

Introduction

Effective synaptic transmission is strongly dependent on vesicle recycling. The family of adaptor protein (AP) complexes, AP-1, AP-2, AP-3 and AP-4, mediates different types of vesicle formation (Boehm and Bonifacino, 2001; Robinson, 2004). The function of the classic clathrin-coated vesicle, AP-2, in synaptic endocytosis is well documented (Slepnev and De Camilli, 2000). In this study, we analyzed a tissue-specific isoform of the AP-1 complex for functions in synaptic vesicle (SV) recycling. Membrane binding of AP complexes is specific, with AP-2 binding exclusively to the plasma membrane and all others to organelles of the late secretory/endocytic routes. Adaptor protein-1 mediates protein sorting between the *trans*-Golgi network (TGN) and endosomes (Reusch *et al*, 2002; Ghosh *et al*, 2003). It consists of four adaptins: γ1 and β1, which interact with accessory proteins, and μ1A and σ1A (Supplementary Figure S1). The μ1A-adaptin that binds cargo proteins is essential for membrane binding and is involved in the regulation of membrane binding (Meyer *et al*, 2000; Ghosh and Kornfeld, 2003; Medigeshi *et al*, 2008; Ricotta *et al*, 2008). In vertebrates, three genes encode the σ1–adaptins: A, B and C (Supplementary Figures S1–S3), and σ1A and σ1B have been detected in proteomic analyses of clathrin-coated vesicles (Baust *et al*, 2006; Borner *et al*, 2006). A function of σ1-adaptins is cargo binding in a hemicomplex with γ1. The hemicomplexes δ/σ3 of AP-3 and α/σ2 of AP-2 also bind cargo proteins (Janvier *et al*, 2003; Doray *et al*, 2007). However, σ1-adaptins differ from σ2 and σ3 in a C-terminal extension, indicating that σ1-adaptins might have additional functions, for example, mediating AP-1-specific mechanisms in vesicle formation (Supplementary Figures S1 and S2). This domain protrudes from the complex and is accessible for interactions (Heldwein *et al*, 2004).

During synaptic transmission, small SVs fuse with the PM to release neurotransmitter. Three main endocytic pathways are considered to participate in SV recycling: 'kiss and run', clathrin-mediated and bulk endocytosis. 'Kiss and run' thought to be working exclusively at very low activity. In this case, vesicles fuse with the plasma membrane only transiently and do not require additional endocytic components to restore protein and lipid identity by the endocytic process (Ceccarelli *et al*, 1973; Aravanis *et al*, 2003; Gandhi and Stevens, 2003). When SVs collapse into the PM, proteins diffuse from the exocytic active zone to the endocytic site, and are endocytosed through clathrin-coated vesicles (Heuser and Reese, 1973; Takei *et al*, 1996; Cremona and De Camilli, 1997; Wienisch and Klingauf, 2006). Adaptor protein-2 together with CLASP proteins could ensure proper sorting of SV proteins during endocytosis (Slepnev and De Camilli, 2000). Compensatory endocytosis by clathrin-coated pits is thought to be the dominant mechanism of membrane retrieval (Lagnado *et al*, 1996; Atluri and Ryan, 2006; Wienisch and Klingauf, 2006; Balaji *et al*, 2008), necessitating efficient sorting of exocytosed vesicle proteins at the PM. Bulk endocytosis occurs only at strong stimulation and endosomal structures formed during this process have to be reformed into small SVs with proper sorting of lipids and proteins. This particular process might involve APs other than AP2. Though involvement of endosomal sorting step during SV recycling is

*Corresponding authors. P Schu, Zentrum für Biochemie und Mol. Zellbiologie, University of Göttingen, Abt. Biochemie II, Humboldt-Allee 23, Göttingen D-37073, Germany. Tel.: +49 551 395 949; Fax: +49 551 395 979; E-mail: pschu@gwdg.de or J Klingauf, Institute of Medical Physics and Biophysics, University of Münster, Robert-Koch-Str. 31, Münster D-48149, Germany. Tel.: +49 8356933; Fax: +49 8363801; E-mail: klingauf@uni-muenster.de
[5]Present address: Max-Planck Institute for Biophysical Chemistry, Department of Neurobiology, Am Fassberg 11, 37077 Göttingen, Germany
[6]These authors contributed equally to this work

Received: 11 May 2009; accepted: 26 January 2010; published online: 4 March 2010

far less well documented (Wucherpfennig *et al*, 2003) and, in fact, heavily debated (Murthy and Stevens, 1998). In early electron microscopy (EM) work by Heuser and Reese (1973), it has been proposed that endocytosed SV might recycle through early endosomes, as they can be observed in large neuromuscular synapses. Yet it does not exclude formation of observed structures by bulk endocytosis. However, endosomal intermediates have been observed less frequently in small synapses, such as hippocampal boutons.

Deficiency in the ubiquitously expressed AP-1 adaptins, γ1 or μ1A, is embryonic lethal. The γ1-deficient embryos cease development at embryonic day 3.5 pc, whereas μ1A-deficient embryos cease development at mid-organogenesis (day 13.5 pc). The observation that μ1A-deficient embryos reach organogenesis is probably due to the homologous μ1B, expressed exclusively in polarized epithelial cells (Meyer *et al*, 2000). In contrast, the ubiquious γ2 cannot complement the γ1 deficiency (Zizioli *et al*, 1999). We generated a targeted mouse 'knock-out' of the X-chromosomal σ1B-adaptin. We found that σ1B-adaptin mediates SV recycling through endosomal intermediates in small hippocampal boutons. This is a new function of AP-1 and the first *in-vivo* function of a σ1 isoform. It demonstrates SV recycling in small synapses through endosomes that might originate from bulk endocytosis. These data reveal a molecular mechanism for a severe human X-chromosome-linked mental retardation (Tarpey *et al*, 2006).

Results

σ1 isoform expression and σ1B-deficient mice

The σ1A, σ1B and σ1C isoforms are found only in vertebrates. One σ1-adaptin gene exists in fly, worm and yeast (Supplementary Figures S2 and S3). The alignment illustrates that ~20 amino acids at the N-terminus and aa 60–120 are highly conserved (pfam 01217). According to the phylogenetic tree, gene diversification occurred during the evolution of vertebrates. This tree is in line with the evolutionary tree of the entire adaptin family (Boehm and Bonifacino, 2001). Tissue-specific mRNA expression of σ1 isoforms was analyzed by northern blot analysis and RT–PCR (Figure 1A–C; Supplementary Figures S5). The *σ1A* mRNA is ubiquitously expressed and is readily detected in all tissues analyzed, but expression is significantly higher in the brain. Expression levels of σ1B and σ1C are highly variable and tissue specific, with most tissues expressing σ1A and only one of the other isoforms (Figure 1A–C; Supplementary Figure S5). The high expression levels of σ1B and σ1A in the brain confirm earlier studies using human tissue samples (Takatsu *et al*, 1998).

A genomic fragment of the X-chromosomal σ1B locus was isolated, mutated, and introduced into the 129SV/J mouse line (Supplementary Figure S4) and crossed with C57/Bl6 animals. The σ1B-deficient mice are viable, whereas, knockouts of γ1 and μ1A are embryonic lethal (Zizioli *et al*, 1999; Meyer *et al*, 2000). Growth and development were normal, but it was noticed that they were calm and had problems finding the water source, when moved between different types of cages. The σ1B deficiency does not alter protein levels of γ2- or μ1A-adaptin and clathrin in fibroblasts, whereas γ1 is reduced by 20%, confirming that adaptins are stable only in a heterotetrameric complex (see Supplementary Figure S7). In addition, mannose-6-phosphate receptor distribution is not altered in σ1B-deficient fibroblasts, in contrast to μ1A-deficient fibroblasts (Meyer *et al*, 2000; Supplementary Figure S8). These data demonstrate that σ1B is not required for ubiquitous, 'house-keeping' functions of AP-1, but mediates tissue-specific AP-1 functions. However, deletion of the σ1B subunit leads to an increase in α-adaptin expression (25%; $P<0.05$) as tested by western blotting on the brain homogenates and mouse embryonic fibroblasts (MEFs; Figure 1D; Supplementary Figure S7). In the brain, however, γ1 expression is normal in σ1B-deficient animals (Figure 1D). Thus in the brain, σ1-adaptin expression is not limiting for complex formation unlike the case in embryonic fibroblasts.

Localization of AP-1 to hippocampal boutons

The ubiquitously expressed AP-1/σ1A complex is predominantly localized to the peri-nuclear TGN, but is also found on endosomes. Moreover, AP-1 deficiency impairs endosomal sorting functions (Meyer *et al*, 2000; Medigeshi and Schu, 2003; Saint-Pol *et al*, 2004). To determine the subcellular localization of AP-1/σ1B complexes, we expressed HA-tagged σ1-adaptins in wild type and σ1B-deficient MEFs. None of them could be unambiguously localized by IFM to either TGN or endosomes, indicating that the C-terminal domains of membrane-bound complexes are masked. Therefore, we used an anti-γ1-adaptin antibody to determine AP-1 localization to hippocampal boutons. The β1-adaptin of AP-1 has been detected in a study identifying and quantifying SV proteins (Takamori *et al*, 2006).

The co-localization of AP-1 with the pre-SV marker, synaptohysin, was tested by high-resolution 4Pi microscopy (Hell *et al*, 1994) and detected in control and σ1B-deficient neurons (Figure 2A). However, no or very little co-localization was observed between AP1 and the post-synaptic marker, Homer, both in WT and knockout boutons; thus supporting a predominantly pre-synaptic localization of AP-1 (Figure 2A). Quantification by distance analysis was performed between the fluorescence centers of patches of either γ- or α-adaptin and synaptophysin or Homer, respectively. Mean distances between γ/α-adaptin patches and synaptophysin were within one and a half SV diameter (from 32 ± 3.9 to 58.8 ± 6.8 nm), whereas those between γ-adaptin and Homer were significantly larger, ranging from 109 ± 16 nm in 'knock-out' to 153.5 ± 29.7 nm in WT (Figure 2B). Such short mean distances between AP-1 and synaptophysin (58.8 ± 6.8 nm for WT and 48.4 ± 5.5 nm for 'ko') indicate the localization of AP-1 within the SV cluster (~300 nm diameter) similar to the AP-2 distribution detected in our experiments. These data are in line with our EM data in which we observe clathrin-coated structures right next to SV clusters (see Figures 3 and 7).

Synaptic vesicle functions in σ1B-deficient neurons

Detailed analysis of presynaptic ultrastructures confirmed our suggestions regarding a possible role of AP-1 in SV recycling. Electron micrographs of hippocampal synapses were prepared to determine SV numbers and their size. Numbers and distribution were determined at rest and after strong stimulation by 900 AP/10 Hz, which results in a considerable depletion of the SV pool (Figure 3A). Even from the first sight one could see the strong phenotype in 'ko' boutons. Although resting synapses from controls contained ~230 SVs per μm^2, σ1B-deficient synapses contained

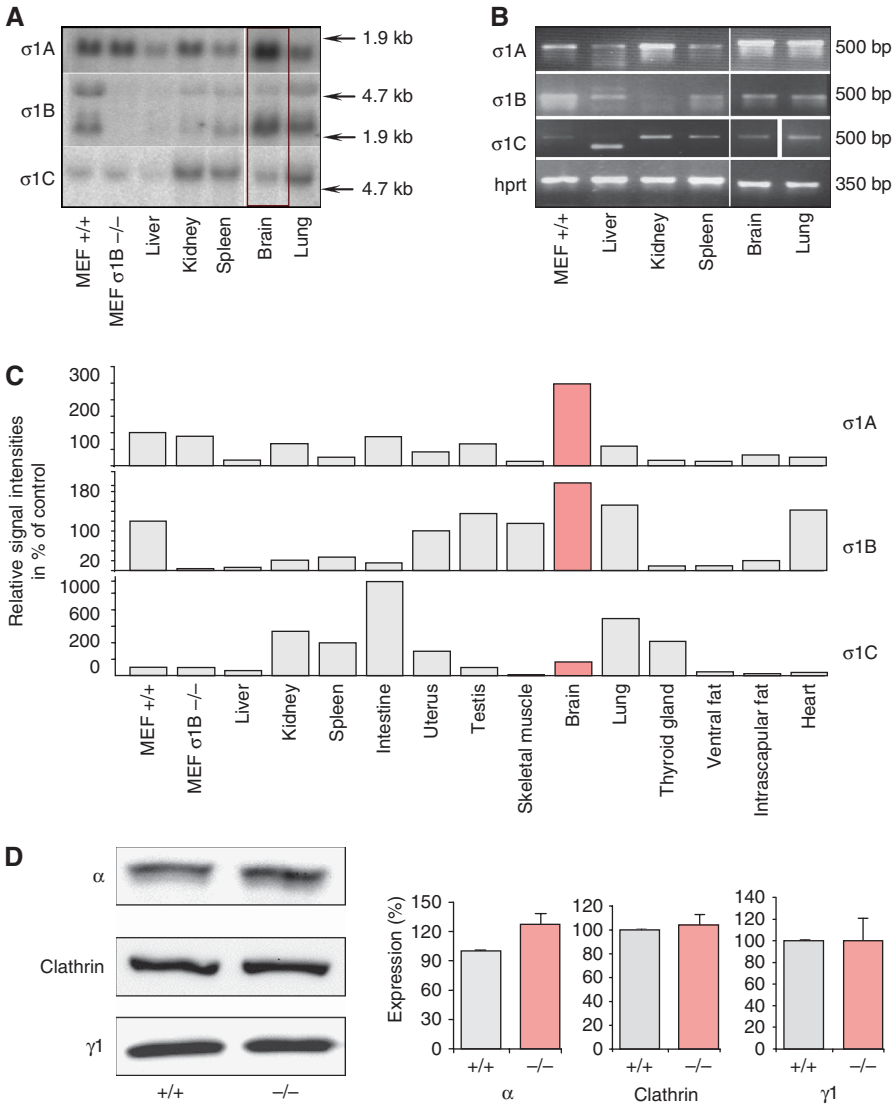

Figure 1 The σ1 isoform tissue-specific expression pattern. (**A**) Expression analysis by northern blots. The expressions of σ1A and σ1C are not upregulated in the σ1B 'knock-out' and are highest in the brain. (**B**) RT–PCR to confirm low expression levels indicated by northern blot analysis. (**C**) Expression levels in all tissues tested (see Supplementary Figure S5 for northern blots and RT–PCR). Northern blot signal intensities were normalized and calculated relative to the signal in mouse embryonic fibroblasts. (**D**) Expression analysis of α- and γ1-adaptins and clathrin in WT and ko brain homogenates performed by western blotting (paired *t*-test, $P<0.05$; three brains per genotype).

only ~135 SVs per μm^2. After depletion of the SV pool in controls, their density was reduced to ~105 SVs per μm^2, whereas depletion in σ1B-deficient synapses reduced SV numbers to only ~47 SVs per μm^2 (Figure 3B). Stimulation of recycling and depletion of the vesicle pool also increases the number of structures with diameters larger than 60 nm (normal SV diameters range from 35 to 45 nm). In σ1B-deficient synapses, these larger organelles were already found more often in resting synapses, whereas strong stimulation led to a further increase in both genotypes (Figure 3C; for more details see Supplementary Table SI). This is also documented by three-dimensional (3D) reconstructions of synapses (Figure 7C and D). In addition, SV from σ1B-deficient neurons were enlarged at rest with diameters of ~41 nm compared with ~38 nm in controls and were more heterogenous (Figure 3D). This indicates that σ1B deficiency reduces the fidelity of SV formation already at rest at basal vesicle-recycling rates. Alternatively, increasing vesicle and quantal size could be a mechanism to compensate for the reduced vesicle numbers. Next, we analyzed the targeting of SV to the active zone and their docking to the PM (Figure 4). Upon stimulation, SV numbers of visibly docked SVs per 100-nm active zone were reduced by 60% in σ1B-deficient synapses compared with only 28% in controls. Even at rest, SV numbers in σ1B-deficient synapses were already reduced by 40% in comparison with controls. We then determined the numbers of all SVs as within a distance of 20 nm to the active zone in σ1B-deficient synapses. We observed these to be reduced to degrees similar to those of docked SVs after stimulation (Figure 4C). Thus, targeting and docking of the SVs formed in σ1B-deficient synapses is very efficient and seems to be able to partially compensate for the reduced number of vesicles. This result cannot be reconciled with a defect in SV biogenesis earlier in the secretory pathway at the TGN.

Analysis of SV in acute hippocampal slices from adult animals revealed a reduction in SV numbers and an increased abundance of profiles >60 nm comparable with those deter-

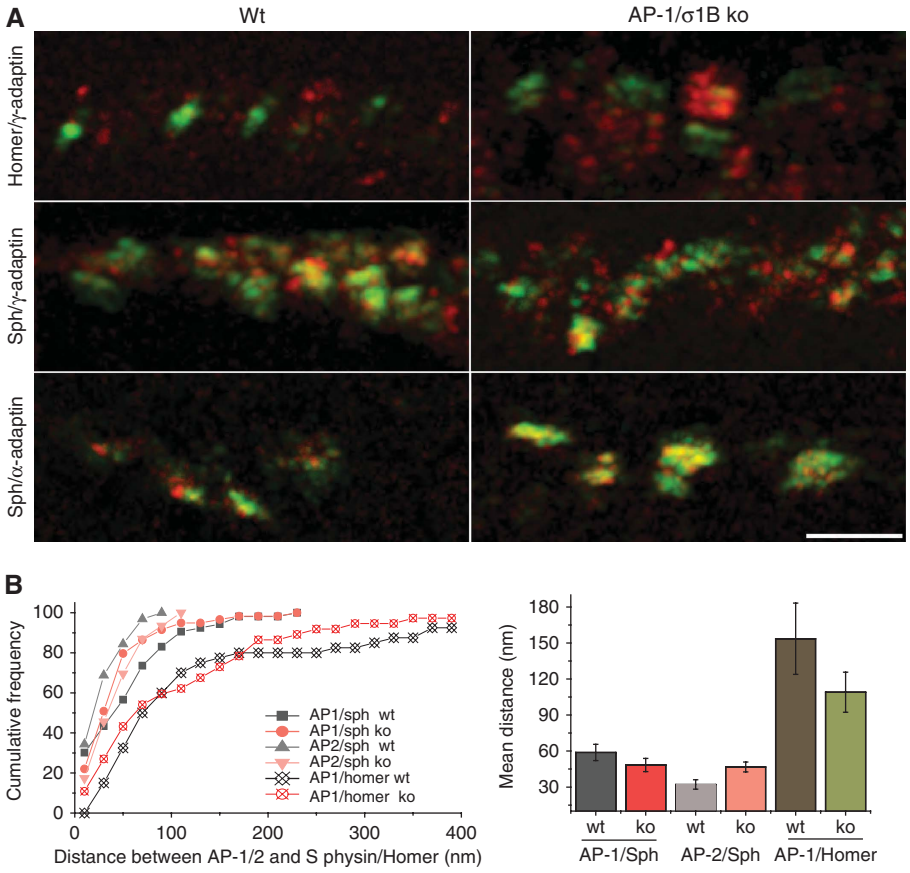

Figure 2 Pre-synaptic localization of AP-1 in WT and ko synapses. (**A**) Representative deconvolved 4Pi microscopy pictures of localization of immunofluorescently labeled α- and γ1-adaptins (in red) relative to post-synaptic marker, Homer, or pre-synaptic marker synaptophysin (in green). Bar 2 μm. (**B**) Calculation of the distances between the centers of the fluorescent signals. Left panel shows the cumulative plot of the distributions of the distances between AP-1/-2 and synaptophysin/Homer. Right panel shows the bar diagram of mean distances.

mined in the cultured neurons isolated from newborn animals (see Supplementary Figures S9 and S10).

Synaptic vesicle recycling and repriming

The observed differences in the SV pool in σ1B-deficient neurons helped us to characterize the kinetics of SV recycling in more detail. Hippocampal neurons from newborn mice were cultured and SV recycling was measured using the exo- and endocytosis probe, synaptopHluorin, a pH-sensitive green fluorescent protein fused to the SNARE synaptobrevin/VAMP2 (Miesenböck *et al*, 1998). Weak stimulation of SV exocytosis by 100 APs at 20 Hz revealed a slight delay in the acidification of endocytosed structures in σ1B-deficient mice (Figure 5A), which was increased by stimulations by 300 APs at 10 Hz (Figure 5B). Next, we quantified SV recycling by measuring the rate of the recovery of the synaptopHluorin response after complete depletion of the total recycling SV pool (Figure 5C). First, a reference test stimulus (100 APs/20 Hz) was applied followed by a depleting stimulus (600 APs/50 Hz). Then, using different delay times, a second test pulse (100 APs/20 Hz) was given and the fraction of recovery was calculated as the paired pulse ratio of the two test pulse fluorescence amplitudes (ΔF2/ΔF1). Within the first 10 s after depleting stimulation, only 46.5% of the exocytosed vesicles become re-available for release in σ1B-deficient neurons compared with 94% in the isogenic controls. Moreover, SV reformation was incomplete in σ1B-deficient neurons, reaching only 70% (Figure 5C). These data demonstrate that the reduction in SV numbers determined in the EM images is caused by a defect in SV recycling.

AP-1 localization in σ1B-deficient hippocampal boutons

The σ1A and σ1B isoforms are highly expressed in the brain. As SV formation is not completely blocked in σ1B-deficient neurons, AP-1/σ1A complexes might also contribute to SV formation in the absence of σ1B. Therefore, we quantified AP-1/synaptotagmin co-localization determined by IFM in hippocampal neurons at rest and after stimulation of SV recycling either using 900 AP/10 Hz or by high potassium concentrations (Figure 6A–D; Supplementary Figure S12). We also determined AP-2 (α) and synaptotagmin co-localization (Figure 6E; Supplementary Figure S11). In wild type neurons, co-localization of either γ1- or α-adaptin did not change on stimulation of SV recycling (Figure 6D and E; Supplementary Figures S11 and S12). However, in σ1B-deficient neurons co-localization of γ1 and synaptotagmin increased significantly on either type of stimulation (Figure 6A–D). Co-localization of α-adaptin and synaptotagmin was not altered (Figures 6D and E; Supplementary Figure S11). The analysis of EM images revealed clathrin-coated buds on the accumulated endosome-like structures. This is shown in the 3D reconstruction of control (Figure 7A and B) and σ1B-deficient synapses (Figure 7C and D). In the panels (A) and (C), SVs were

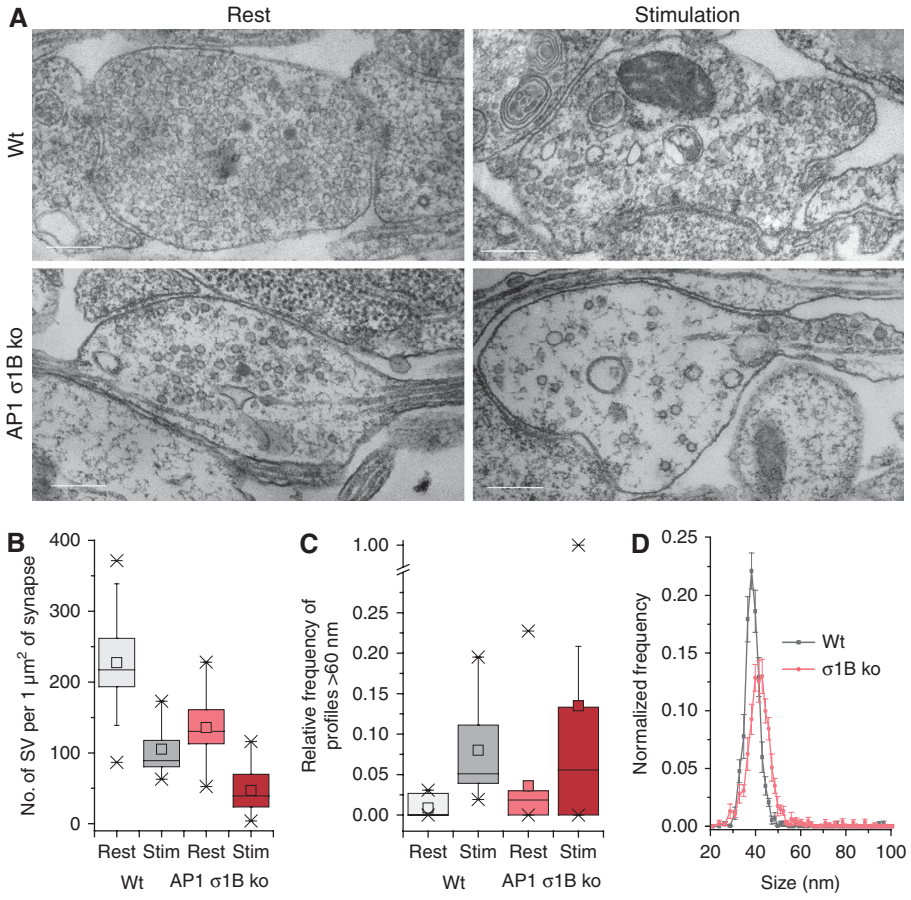

Figure 3 Synaptic vesicle numbers and size. (**A**) Electron microscopic images of hippocampal boutons taken at rest and after stimulation with 900 AP/10 Hz. Scale bar: 200 nm. (**B**, **C**) Quantification of synaptic vesicle (SV) numbers and of the accumulation of membranous structures with diameters larger than 60 nm (s.e.m.; see Supplementary Table SI). Box plots represent: smallest and the largest outliers; lower and upper 'whiskers', smallest and largest non-outlier observations, correspondingly; lower quartile, median and upper quartile; mean value (Origin 7.5, OriginLab Corp.). (**D**) Distribution of SV diameters at rest (s.e.m.; see Supplementary Table SI).

excluded for better visibility (for more details, see Supplementary Movies S1 and S2). Endosome-like structures accumulating in the σ1B-deficient synapses are coated with clathrin that are most likely recruited by AP-1/σ1A complexes. Thus, the increased γ1/synaptotagmin co-localization on stimulation of SV recycling seems to be caused by the impaired SV reformation from accumulated endosomal structures in the absence of σ1B. However, increased expression of α-adaptin (Figure 1D) adequately correlates with the increased number of clathrin-coated vesicles in the knockout synapse.

Behavioral alterations of σ1B-deficient mice

Behavioral testing of the mice revealed that they are hypoactive (Figure 8A). However, neither ambulatory nor qualitative exploratory measures were significantly different in the open-field test (data not shown). Motor coordination and balance were tested on an accelerating rotarod. Although grip strength was normal, the σ1B-deficient animals were unable to learn to balance (Figure 8B). This defect might be attributed to hypoactivity or impaired motor learning ability, but apparently not to a proper ataxic phenotype, as swimming velocity and endurance in the water maze were not altered (data not shown). Spatial learning and memory was tested in the hidden-platform Morris water maze, which in mice is mediated by the hippocampal formation (Bird and Burgess, 2008). Notwithstanding their normal swimming ability, σ1B-deficient animals failed to develop a clear preference for the hidden-platform position, during the acquisition trials (genotype effect $P<0.001$; Figure 8C; for details on training period, see Supplementary Figure S13). Most notably, mutants used consistently longer swimming paths to reach the platform ($P<0.001$; data not shown), which again indicates that the deficit could not be reduced to neuromotor impairment. These phenotypes of the σ1B-deficient mouse match a disease in humans, which was linked to the X-chromosomal σ1B locus. Patients carrying premature STOP codons have a severe mental retardation, learn to walk only at 4–6 years, do not develop any intelligible speech and require lifelong comprehensive care (Tarpey *et al*, 2006).

Discussion

σ1-adaptin functions

Thus far three attempts have been made to generate AP-1 'knock-out' mice. Only the σ1B 'knock-out' mouse is viable and fertile, whereas 'knock-outs' of the ubiquitously expressed γ1 and μ1A isoforms are embryonic lethal at early stages. The μ1A-deficient embryonic fibroblasts cell lines could be established, demonstrating that AP-1 is essential

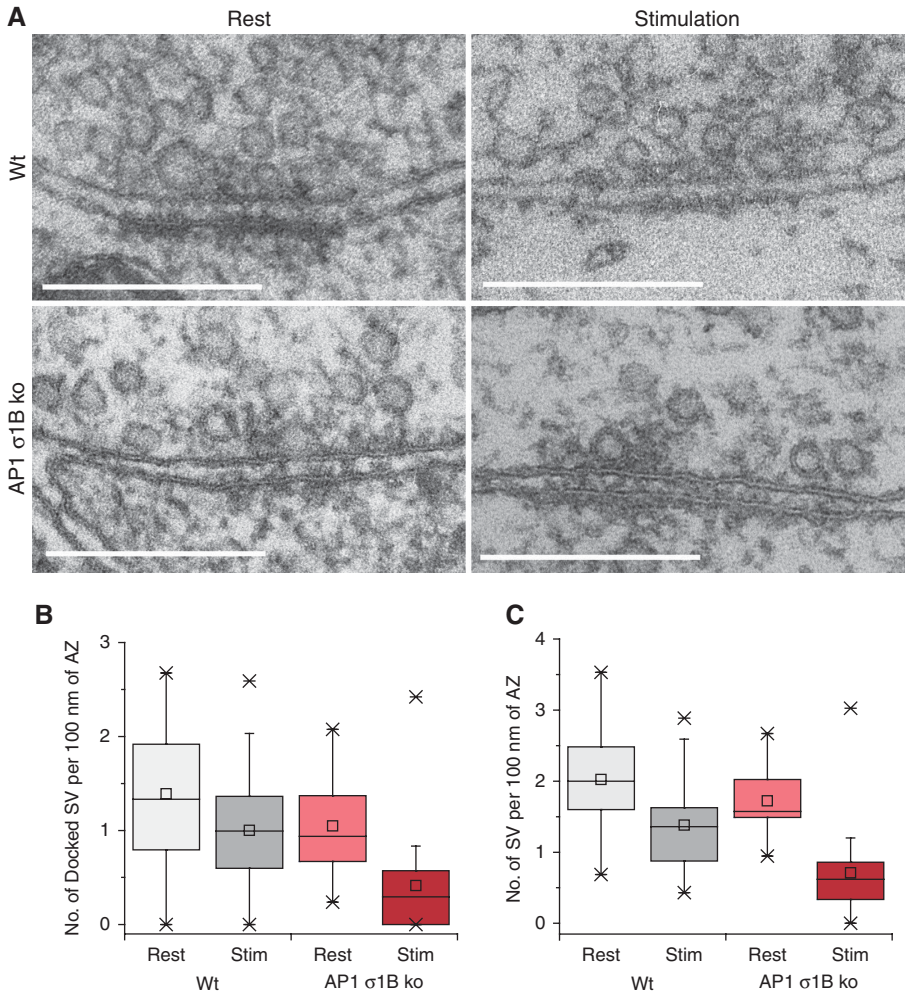

Figure 4 Targeting of synaptic vesicles to the active zone (AZ). (**A**) Exemplar electron micrographs of AZs of synapses from control and $\sigma1B^{-/-}$ animals. Scale bar: 200 nm. (**B**, **C**) Numbers of docked SVs and those within a distance of 20 nm from the AZ membrane. Hippocampal boutons of control and $\sigma1B^{-/-}$ animals at rest and after stimulation (900 AP/10 Hz). Both normalized per 100 nm of AZ; s.e.m., see Supplementary Table SI). For box plot description, see legend of Figure 3.

for *in utero* development, but not for cell viability (Zizioli *et al*, 1999; Meyer *et al*, 2000). Viability of σ1B-deficient mice and the tissue-dependent σ1B expression pattern demonstrate that it is not required for ubiquitous, 'house-keeping' AP-1 functions, but is expected to mediate tissue-specific AP-1 functions. The σ1B-deficient mice are hypoactive, display deficits in neuromotor learning and spatial learning and memory tasks. These data support a genetic screen in humans for analyzing X-chromosome-based diseases that link the σ1B locus to severe mental retardation (Tarpey *et al*, 2006). These patients learn to walk only at 5–6 years of age, do not develop any intelligible language and require lifelong comprehensive care.

The σ1 subunit is present in three isoforms: A, B and C. The σ1 isoforms differ from their closest homolog, σ2, in having a C-terminal extension and their sequences differ in this region. This domain elongates an α-helix, also seen in σ2, whereas the 10 terminal residues are unstructured. This domain protrudes from the complex pointing toward the membrane (Collins *et al*, 2002; Heldwein *et al*, 2004). Therefore, it could bind to other proteins involved in protein sorting and vesicle formation. Most of those, collectively called, 'accessory' proteins bind to the 'ear' domains of the large adaptins. The σ1-adaptins may thus interact with additional, yet unidentified proteins (Schmid and McMahon, 2007). We observe the σ1-isoforms, B and C, to be expressed in a tissue-specific manner, whereas σ1A is ubiquitously expressed, with remarkably elevated expression in the brain. Furthermore, σ1B expression is highest in the brain. This is in agreement with the distribution of γ1-adaptin in the mouse brain as documented in Allen Mouse Brain Atlas (Supplementary Figure S6) with highest expression in hippocampus; moreover, using high-resolution 4Pi microscopy, we localized AP-1 primarily to the pre-synapse. We observed the number of SVs to be reduced at rest in small hippocampal boutons and to be markedly reduced after turnover of the entire SV pool. This could be caused by defects in SV recycling or by a defect in SV biogenesis, generating vesicles with impaired recycling rates. However, we observed SV to be efficiently targeted to the active zone, which cannot be reconciled with a defect in vesicle biogenesis. The defect in SV recycling observed in the synaptopHluorin experiments, the accumulation of large membranes, not connected to the PM and carrying clathrin-coated buds, together with the

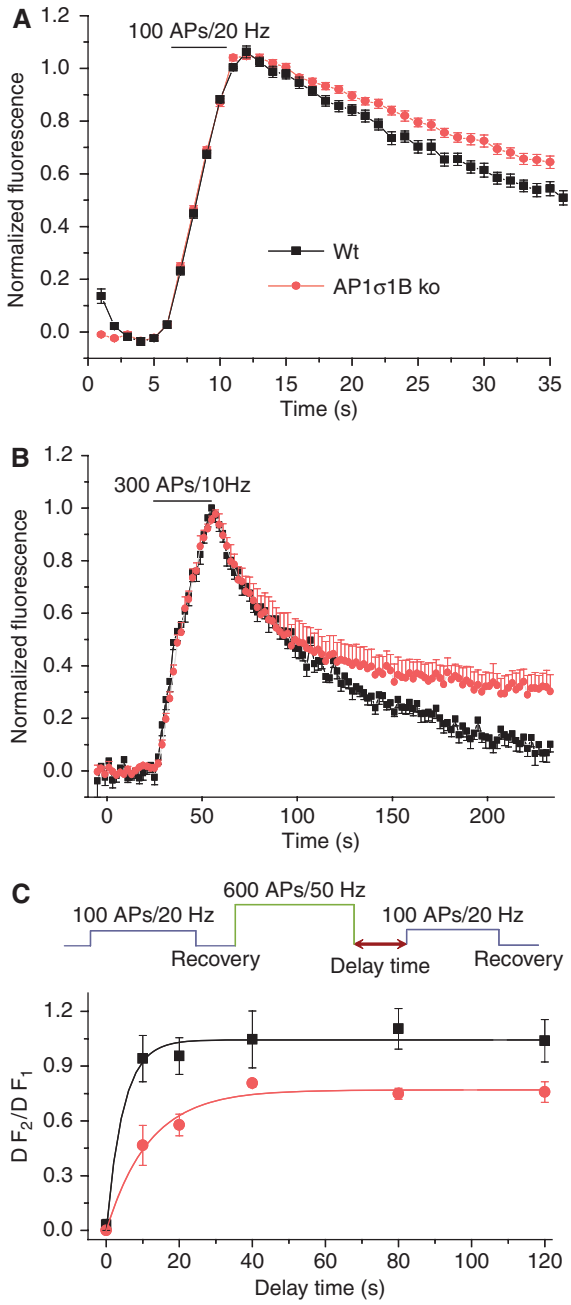

Figure 5 Impaired recycling and acidification of synaptic vesicles in hippocampal boutons of $\sigma1B^{-/-}$ animals. (**A**, **B**) Reacidification after stimulation at 100 AP/20 Hz (s.e.m., see Supplementary Table SI) and at 300 AP/10 Hz (s.e.m., see Supplementary Table SI). (**C**) Delayed SV re-priming after full depletion of the total recycling SV pool by 600 AP/50 Hz stimulation. Upper panel shows the protocol of stimulation, consisting of a reference test pulse (100 APs/20 Hz), a depleting stimulus (600 APs/50 Hz) and at a variable delay time, Δt, a second test pulse (100 APs/20 Hz) to probe recovery as the fraction of test pulse fluorescence amplitudes ΔF2/ΔF1. Within the first 10 s after stimulation, only 45% of exocytosed material was retrieved compared with 90% in wild type controls (s.e.m.; see Supplementary Table SI; average of 30 boutons per region were counted).

pre-synaptic localization of AP-1 accompanied by an increase in AP-2 expression might suggest AP-1/σ1B function on disassembly of 'bulk' endocytic structures.

AP-1-dependent SV recycling

Recycling of SV is fast and models try to include only a limited number of vesicle budding and fusion steps. The 'kiss-and-run' model involves only fusion pore opening, without membrane fusion, avoiding subsequent protein sorting (Wu *et al*, 2007). Its existence is highly controversial, and also it could not account for the high protein and membrane turnover rates under stronger stimulation. Clathrin-mediated endocytosis (CME) occurs at the PM. Protein sorting at the PM could be achieved by AP-2, 'clathrin-associated-proteins' (CLASP) and 'accessory' proteins (Slepnev and De Camilli, 2000). The requirement of endocytosis mediated by clathrin, AP-2, CLASP and accessory proteins has been demonstrated in many systems (Wenk and De Camilli, 2004; Jung and Haucke, 2007). The AP-1 complexes have been detected on endosomes, besides the TGN, where most of membrane-bound AP-1 is detected. Therefore, AP-1/σ1B dependence strongly indicates SV recycling through endosomes. On the basis of the current knowledge, AP-1/σ1B-mediated SV formation from bulk membrane invaginations would also be possible, if these acquire endosomal membrane characteristics. This could be achieved by fusion of these membranes with a minute early endosome and the subsequent maturation of the internalized PM domain into an endosomal membrane. Support for formation through bulk endocytosis comes from recent knockdown experiments (Kim and Ryan, 2009). Knockdown of μ2-adaptin (AP-2) by siRNA lead only to slowing, but not elimination of endocytosis, with the remaining component relying mostly on AP-1. Thus, AP-1 might figure in a bulk endocytic retrieval mechanism. However, there is not much evidence for bulk endocytosis in small central nervous system synapses as a compensatory mechanism for a saturated AP-2/clathrin pathway (Wu *et al*, 2007) for mild stimuli, as used here, in contrast to stimulation by continuous depolarization with high K^+ level.

Recently, the analysis of lipid and protein composition of an average SV revealed an unexpectedly high protein content and demonstrated that nearly all proteins are present in excess (Takamori *et al*, 2006). This raises the question, whether high sorting fidelity is even required during recycling. The high copy numbers could ensure that each vesicle obtains a sufficient number of any SV proteins. The resulting high concentration of sorting motifs increases endocytosis rates because of more efficient AP recruitment (Meyer *et al*, 2001). Sorting events during endocytosis mediated by AP-2, in concert with CLASPs, can increase sorting fidelity (Slepnev and De Camilli, 2000). Only H^+–ATPase is present at mere 1–2 copies per vesicle (Takamori *et al*, 2006). Its sorting into a vesicle during endocytosis might be inefficient and acidification of a larger, endosomal intermediate and subsequent AP-1/σ1B-mediated SV budding would ensure the formation of a large acidified vesicle pool. Thus, AP-1/σ1B-mediated SV formation from endosomal intermediates could contribute to SV recycling at high turnover rates; whereas AP-2- and clathrin-mediated endocytosis would be sufficient to regenerate SV precisely at the PM. The involvement of AP-1/σ1B could thus be considered as a resynthesis of SV, whereas AP-2 mediates recycling through CME only.

However, our EM data on synapses from hippocampal slices indicate that SV reformation by AP-1/σ1B from endosomes is a frequently taken route.

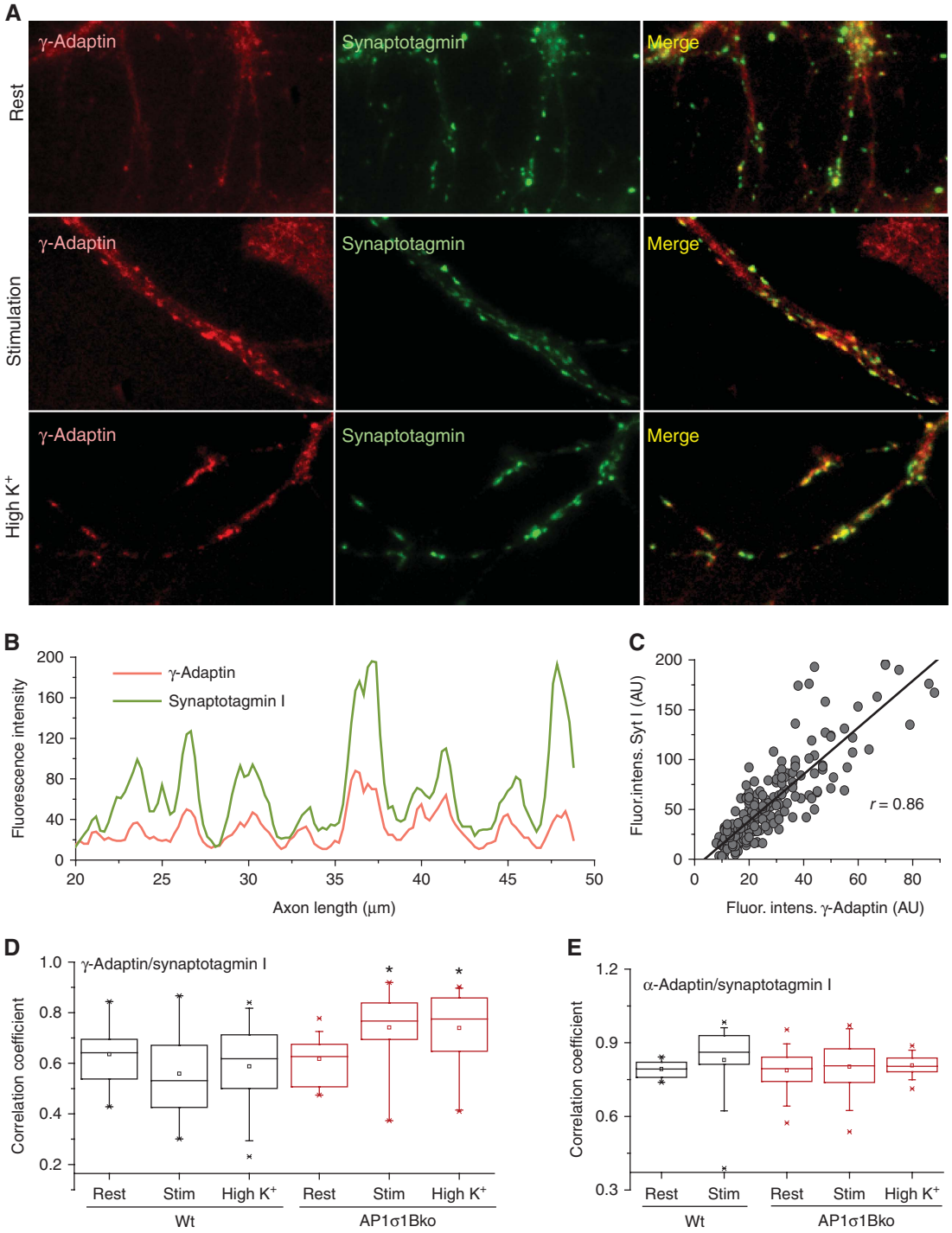

Figure 6 Stimulation-dependent co-localization of AP-1 and synaptotagmin 1 in σ1B-deficient neurons (controls see Supplementary Figures S11 and S12), determined at rest and after stimulation with 900 AP/10 Hz or by 90 mM K^+ for 1 min. (**A**) Representative immunofluorescence images. (**B**) Co-localization along an axon. (**C**) Degree of co-localization (axes are fluorescence intensity in arbitrary units). (**D**, **E**) Quantification of γ1-adaptin/synaptotagmin 1 (s.e.m.; see Supplementary Table SI) and α-adaptin/synaptotagmin 1 (s.e.m.; see Supplementary Table SI) co-localizations in control and σ1B-deficient synapses at rest and after stimulation. For box plot description, see legend of Figure 3. For each box plot, at least 10 axons were analyzed; correlation coefficients for γ1-adaptin/synaptotagmin 1 co-localization in σ1B-deficient synapses after stimulation are significantly higher (pared *t*-test, $P<0.05$; large asterisks).

AP-1-dependent SV biogenesis

One could expect the involvement of AP-1/σ1B even in the biogenesis of SV at the TGN or at a somatic endosomal compartment. The slight reduction in SV numbers in synapses at rest and the efficient targeting of SV to the active zone indicate an un-impaired SV biogenesis. The expression of σ1A is highest in the brain, further indicating a crucial function of the ubiquitously expressed AP-1/σ1A in SV protein sorting. This is supported by the increased γ1 co-localization with synaptotagmin and the accumulation

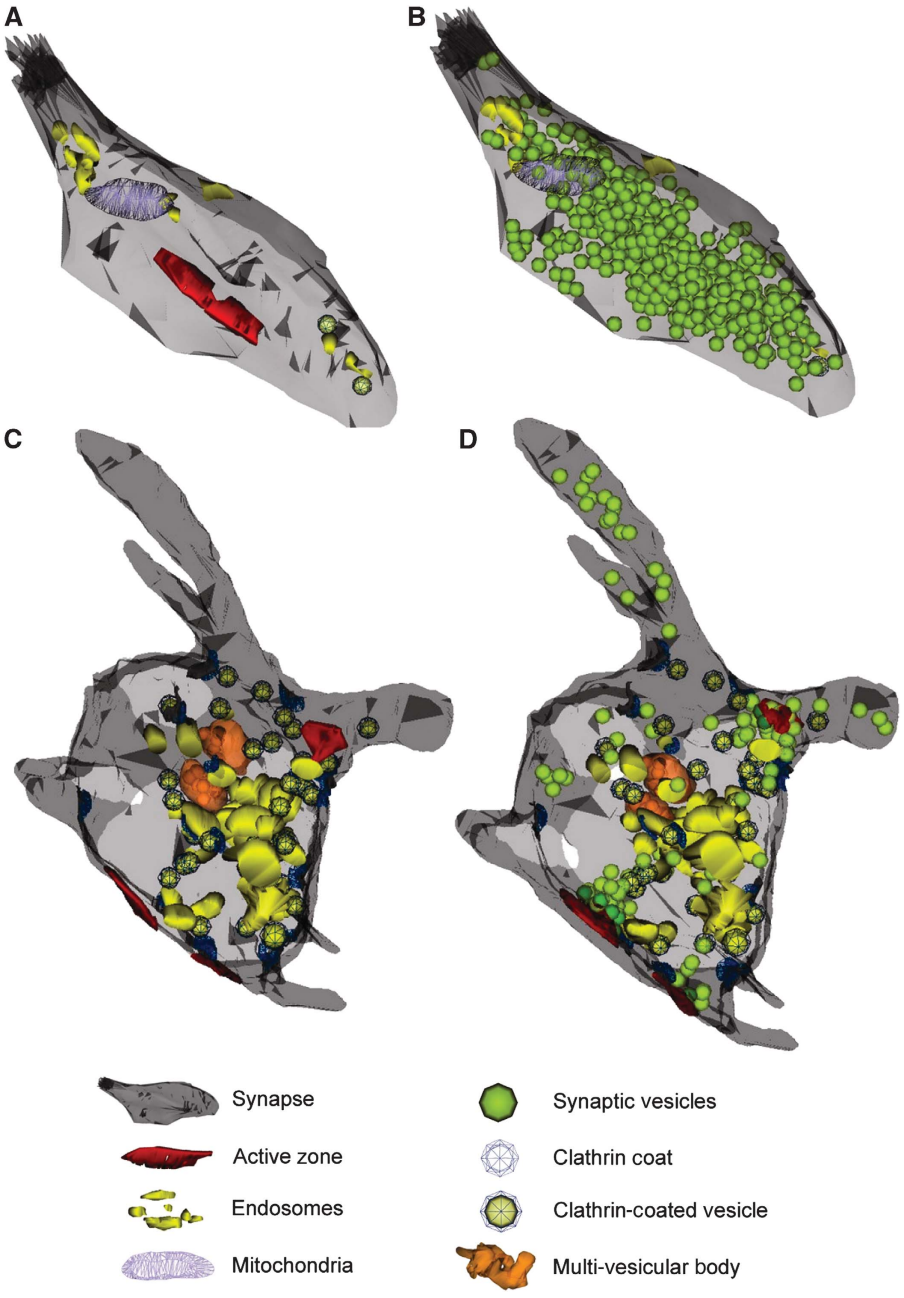

Figure 7 Accumulation of endosome-like structures and clathrin coats. 3D-reconstruction of synapses from (**A**, **B**) wild type and (**C**, **D**) σ1B-deficient synapses. In (**A**) and (**C**) synaptic vesicles are excluded (see also Supplementary Movies S1 and S2).

of endosomal clathrin coats in σ1B-deficient synapses on stimulation. Mixed AP-1/σ1A–AP-1/σ1B coats could form, as the major AP-1 membrane-targeting information seems to reside in the γ1-adaptin and its putative PI-4-P-binding motif (Wang *et al*, 2003). Moreover, if biogenesis of SV, or just a subtype of SV solely formed by AP-1/σ1B, would be blocked, a more severe phenotype is expected. The absence of VGLUT1 or VGLUT2 is lethal post-nataly. Both are expressed in the same hippocampal synapses in the first weeks after birth and they reside in the same vesicle (Fremeau *et al*, 2004; Wojcik *et al*, 2004; Herzog *et al*, 2006; Moechars *et al*, 2006). At the TGN, SV biogenesis occurs at a much lower rate than that at endosomes during SV recycling. The major difference between biogenesis and recycling seems to be the rate at which SVs are formed. The AP-1/σ1A complexes seem to be able to mediate SV biogenesis on TGN membranes and, at a low rate, even independent of AP-1/σ1B on endosomes, whereas AP-1/σ1B is crucial during recycling through endosomes.

AP-dependent synaptic protein sorting

The neuron-specific AP-3B complex was first shown to be involved in SV formation, whereas the ubiquitous AP-3A is not. Both share the δ-adaptin, whereas their other subunits differ (Newell-Litwa *et al*, 2007). Defects in SV recycling and biogenesis are observed in mice lacking both AP-3A and AP-3B (Kantheti *et al*, 1998; Voglmaier *et al*, 2006). Newborns are hypopigmented and have balancing problems.

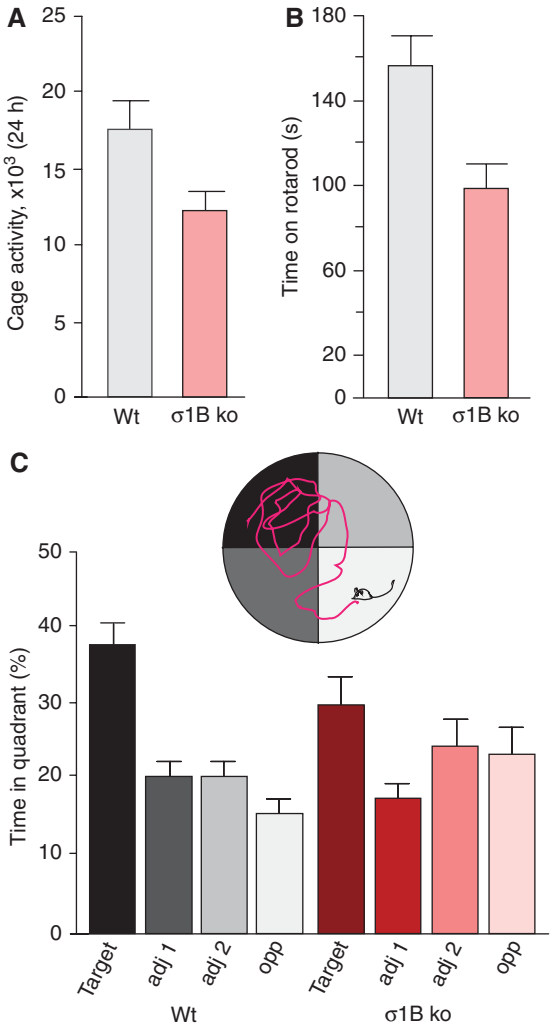

Figure 8 Behavioral testing. Hypoactivity, impaired motor coordination and reduced hippocampus-dependent spatial memory in $\sigma1B^{-/-}$ animals. (**A**) Cage activities of individual animals expressed as numbers of light beam crossings within 24 h (s.e.m.). (**B**) Motor coordination expressed as the time animals can balance on rotating, accelerating bar (s.e.m.; rotarod). (**C**) Morris water maze to test spatial, long-term memory. Mice learn to find an invisible platform hidden under the water surface to rest on. The circular tank is separated in quadrants and the time an animal spends in each quadrant is measured (s.e.m.). Target, quadrant with the hidden platform; adj1 and adj2, neighboring quadrants; opp, opposite quadrant. $\sigma1B^{-/-}$ animals performed normally in the training period (see Supplementary Figure S13).

However this regresses and mice will be able to stand up on their hind limbs. Deficiency in only AP-3B (μ3B 'knock-out') has a milder phenotype. Mice are hyperactive and GABA vesicle biogenesis, but not recycling, in inhibitory synapses is reduced. This indicates synergistic effects in AP-3A/AP-3B-deficient mice and functions of both in synapse development rather than in SV recycling (Nakatsu *et al*, 2004).

Adaptor protein-4 is required for basolateral sorting (Simmen *et al*, 2002). The AP-4-deficient mice have impaired motor coordination and AMPA receptors are found in autophagosomes in axon shafts and not in dendrites (Matsuda *et al*, 2008).

Our findings strongly indicate that SV recycling, in parallel to CME, heavily depends on an endosomal route that requires the tissue-specific AP-1/σ1B complex in vertebrates. Although γ1/σ1B and γ1/σ1A hemicomplexes might bind different subsets of cargo proteins, various C-terminal domains of σ1-adaptin isoforms seem to fulfill additional functions in the vesicle formation process, which are unique to AP-1- mediated vesicle formation. Their position in the heterotetrameric complex would allow binding to accessory proteins that need to be identified and characterized.

Materials and methods

Molecular biology

Total RNA was reverse-transcribed to cDNA using an oligo-dT primer (Qiagen RT kit). Transcripts for σ1-adaptins were amplified: σ1A: PSS1-6 5′-CGGGATCCTGCAGGATGATGCGATTCATGCT-3′ and PSS1-535 5′-CGGGATC-CTGACGGGGCTATGCCAGGCCC-3′; σ1B: PSRS1-1 5′-CGGGATCCCCCGCGGCCCGCAGCCGCC-3′ and PSRS1-640 5′-CGGGATCCGGAGGACAGTTATGTCA-GTCC-3′; and σ1C: σ1cD2B 5′-CTCTGGATCCGGGGCCATGATACATTTCATC-3′ and σ1cU2SX 5′-CCTCGAGTCGACTGTACACTTAAAACG-3′. Hypoxanthine-phosphoribosyltransferase (HPRT) was amplified as control: HPRT-f: 5′-CCTGCTGGATTAC-ATTAAAGCACTG-3′ and HPRT-r: 5′-GTCAAGGGCATAGCCAACAACAAAC-3′. Genomic fragments of the σ1B locus were isolated from a mouse phage DNA library in EMBL3 and characterized. The neo^R expression cassette from pMC1neopA (Stratagene) was cloned into the *Bam*HI site introduced into exon 3. Construct was linearized by *Not*I and electroporated into the 129SV/J cell line ES 14-1. Mutated ES cells were injected into day 3.5 pc blastocysts that were transferred into foster mothers. Male chimeras were mated with C57/Bl6 (outbred) and 129SV/J (outbred). Mice strains were kept in a central animal facility of the University of Göttingen.

Isolation of RNA

All preparations were carried out according to the RNeasy protocol (Qiagen, Germany) using the following details: for isolation of total RNA, organs were homogenized using an ultra-turrax. A total of 100–200 mg was mixed with 600 μl buffer RLT, homogenized with a rotor–stator homogenizer and centrifuged for 3 min at 8000 *g* at room temperature (RT). A volume of 500 μl aqueous phase was transferred and mixed with the same volume of 70% ethanol and the pellet was re-suspended in 350 μl RLT buffer. Alcoholic solutions were pooled and loaded onto an RNeasy Mini spin column. Subsequent steps were carried out according to the protocol supplied by the manufacturer. For preparation of northern blots, 10 μg RNA was separated by agarose gel electrophoresis and transferred to a nylon membrane.

Hippocampal cell culture

Primary hippocampal neurons were isolated from P0–P2 pups of wild type or AP1-σ1B-deficient mice, dissociated by trypsin digestion and plated on Poly-D-lysine-coated glass coverslips. The neurons were cultured *in vitro* for 12–16 days in NBA medium (Gibco) supplemented with B27 (Gibco), glutamax (Gibco) and PenStrep (Sigma). On 4–5 DIV, cells were transfected with synaptopHluorin construct using a modified calcium phosphate transfection procedure (Wienisch and Klingauf, 2006).

Quantitative synaptopHluorin imaging and analysis

Neurons grown on coverslips were mounted in a laminar flow perfusion chamber on the movable stage of an inverted microscope (Axiovert 200M, Zeiss Oberkochen, Germany) and imaged using a ×63/1.2 W objective (C-Apochromat, Zeiss). The microscope filter set consisted of a beamsplitter 495DCLP and an emission filter HQ560/40 (AHF Analysetechnik, Tübingen, Germany). Epifluorescence was excited using a monochromator (Polychrome IV, TILL Photonics, Germany) with 10-nm bandwith at 475 nm. Cells were perfused with a modified Ringer solution containing 140 mM NaCl, 2.4 mM KCl, 2.5 mM $CaCl_2$, 1.3 mM $MgCl_2$, 10 mM HEPES and 10 mM glucose (290 mOsm, pH 7.3). For electric field stimulation, 10 mM 6-cyano-7-nitroquinoxaline-2, 3-dione (CNQX) and 50 mM D, L-2-amino-5-phosphonovaleric acid (APV; both from Tocris Cookson, Ellisville, USA) were added to saline solution to prevent recurrent activity. Electric field stimulation was performed by

applying 1-ms pulses (constant current source, stimulus isolator A 385, WPI) of 50 mA with alternating polarity delivered by platinum–iridium electrodes spaced at 10 mm. Fluorescence images were taken using an intensified 12-bit cooled CCD camera (PentaMAX, Princeton Instruments, Monmouth Junction, USA), with effective pixel size of 15 μm, driven by the PC-based Metamorph image acquisition program (Universal Imaging Corporation, Downingtown, USA). Quantitative measurements of fluorescence intensity at individual synapses were obtained by averaging a 4×4 area of pixel intensities centered at the optical center of mass of a given fluorescent punctum. Individual puncta were semi-automatically selected using custom Igor (Wavemetrics, Oregon, USA) routine. Large puncta, typically representing clusters of smaller synapses, were excluded.

Electron microscopy

Primary cultures of hippocampal neurons were prepared from wild type or knockout mice at postnatal days 0–2, as described previously. On 12–13 DIV, cells were fixed overnight at 4°C in 0.1 M cacodylat buffer containing 2.5% glutaraldehyde, 1% paraformaldehyde and 0.3% tannic acid (all Sigma, USA). After three washes in cacodylat buffer, cells were post-fixed with 2% osmium tetroxide (Electron Microscopy Sciences, USA) at RT for 1 h, washed extensively with deionized distilled water and stained with 1.5% uranyl acetate. Cultures were then embedded in Epon 812 (Electron Microscopy Sciences) after dehydration in an ethanol series. Ultrathin sections (~60 nm) were collected on Formvar-coated nickel grids and viewed using a Zeiss EM912 electron microscope, photographed at a final magnification of ×30 000 and scanned for later analysis on a flatbed scanner Epson 4990 with 2400 dpi resolution. Morphological analysis was performed with Metamorph software (Molecular Devices, Downingtown, PA, USA).

Immunofluorescence staining

Cells grown on glass coverslips were rinsed twice in PBS (137 mM NaCl, 2.7 mM KCl, 8 mM Na_2HPO_4 and 1.5 mM KH_2PO_4) and then fixed overnight at 4°C in 4% paraformaldehyde in PBS (Sigma). High-potassium stimulation of the cells was performed with a modified Ringer solution containing 90 mM KCl applied for 60 s. Electric-field stimulation was performed as for synaptopHluorin experiments (900 AP at 10 Hz were applied). For both types of stimulation, 10 mM CNQX and 50 mM APV were added to saline solution to prevent recurrent activity. Cells were fixed immediately after the end of stimulation. After three washes in PBS, cells were permeabilized with 0.01% saponin (Sigma) in PBS for 3 min at RT. Fixed cells were then blocked for at least 45 min by incubation with 'blocking buffer' (PBS containing 3% bovine serum albumin and 2% goat serum (both Sigma)) and labeled overnight at 4°C with primary antibodies in 'blocking buffer' in a humidified environment. The dilution factors were 1:300 for antibodies against cytoplasmic epitopes of synaptotagmin 1 (Synaptic Systems, Göttingen, Germany) and 1:100 for anti-γ-adaptin and anti-α-adaptin (BD Pharmingen, Heidelberg, Germany). After washing for 45 min with several changes of 'blocking buffer' solutions, cells were incubated for 1.5 h with appropriate secondary antibodies labeled with Alexa-488, 546 or 594 (1:500 in 'blocking buffer'; Molecular Probes). Then specimen was rinsed with PBS and mounted on a glass using anti-fade mounting medium. Cells were viewed using an inverted epifluorescence microscope (Axiovert 200M). The filter set consisted of a dual band beamsplitter FITC/Texas Red and a dual band emission filter FITC/Texas Red (AHF Analysetechnik, Tübingen, Germany). Images were recorded digitally and analyzed using MetaMorph software (Universal Imaging Corporation).

Correlation analysis of co-localization of α-daptin, γ-adaptin and synaptotagmin 1 was performed using MatLab (The MathWorks, USA) software. In short, the degree of co-localization of the different fluorescent proteins was estimated by cross-correlating position-dependent intensity traces. The parameter K is defined as

$$K = \frac{\langle \delta F(x) \cdot \delta G(x) \rangle}{\sqrt{\langle \delta F(x)^2 \rangle \langle \delta G(x)^2 \rangle}} \text{ with } \langle F(x) \rangle = \frac{1}{2X} \int_{-X}^{X} F(x) \mathrm{d}x$$

and $\langle F \rangle$ denoting the mean of the function F. The significance level for separating different K values was evaluated by a paired t-test. All significant differences can be separated by a probability of more than 95%.

4Pi microscopy

Cells were stimulated for 3 min with 40 mM K^+ solution and proceeded further as for regular immunofluorescence studies; the dilution factors were 1:200 for antibodies against Homer (Synaptic Systems), 1:500 for anti-γ-adaptin, anti-α-adaptin (BD Pharmingen) and synaptophysin (Synaptic Systems). Then cells were covered with 20 μl PBS and sealed using a second cover slip with immobilized red fluorescent beads of subresolution size (TransFluo-Spheres, NeutrAvidin-labeled microspheres, 0.1 μm: excitation maximum: 488 nm; emission maximum: 605 nm), resulting in a space of less than 30 μm between the two covers lips.

Images were obtained with a commercial 4Pi microscope (TCS 4Pi microscope of type A, Leica Microsystems, Wetzlar, Germany) using water immersion lenses (×63, NA 1.2). For two-photon excitation, a mode-locked Ti:Sapphire Laser (MaiTai, Spectra Physics GmbH, Darmstadt, Germany) with pulse length stretched to 1.2 ps was used. The laser was tuned by a grating to a wavelength between 790 and 820 nm. The beam expander was set to 3. Fluorescence originating from the sample was passed through a filter cube (SP700, BS560, BP500–550 and BP607–683), and its intensity was measured using photon-counting avalanche photodiodes (PerkinElmer, Waltham, MA, USA). The detection pinhole was set between 0.77 and 0.86 Airy unit. Samples were mounted between two objectives, and focus and phase of the counter-propagating beams were pre-aligned to the immobilized beads. Then *xz*-stacks of the cells were recorded with a pixel size between 15×15 nm and 25×25 nm in *xz*-direction and a step size of 97 nm. The 4Pi raw images were linearly brightened, rescaled and linearly filtered by a Gaussian Blur using the image processing program ImageJ (Wayne Rasband, National Institutes of Health, USA, http://rsb.info.nih.gov/ij). The distance between two different epitopes was determined using a routine that provides for a elliptical true two-dimensional (2D) fit combined with a tool for distance measurements (commercial plugin for ImageJ, ILTracker, Ingo Lepper Software/Consulting, Münster, Germany). A detailed description of this analysis has been published recently (Hüve *et al*, 2008). Owing to the improved resolution in *z*-direction, for the analysis only the distances in *z*-direction were taken into account. For 3D reconstructions, ghost images, which arise in 4Pi microscopy because of side lobes of the PSF, were eliminated by deconvolution using Leica software, which is based on a linear three-point or five-point deconvolution. Furthermore, reconstructions were then derived from image stacks using the Leica software.

Behavioral testing

Tests were performed on 4-month old female animals, 21 'knockouts' and 15 WT animals. Cage activity was recorded using a lab-built activity logger connected to three IR photo beams. Mice were placed individually in 20×30 cm^2 transparent cages located between the photo beams. Activity was measured over 24 h, expressed as number of beam crossings.

Motor coordination and balance were tested on an accelerating rotarod (MED Associates, St Albans, VT, USA). Mice were trained at constant speed (4 r.p.m., 2 min) before four test trials (inter-trial interval, 10 min). During the test trials, animals balanced on a rotating rod that accelerated from 4 to 40 r.p.m. in 5 min and time until they dropped was recorded; results of four test trials were averaged and expressed as mean latency ± s.e.m. Grip strength was measured using a T-shaped bar connected to a digital dynamometer (Ugo Basile, Comerio, Italy). Mice grabbed the bar and pulled backwards until they released the bar (10 measurements were included for each animal).

A spatial memory version of the Morris maze test was performed in a 150-cm circular pool filled with water at 26°C and opacified with non-toxic paint. A 15-cm round platform was hidden 1 cm beneath the surface. Daily trial block consisted of four swimming trials. Mice that failed to find the platform within 2 min were guided to the platform, where they remained for 15 s. During probe trials, the platform was removed and the search pattern recorded for 100 s. Swimming paths of the animals were recorded using EthoVision video-tracking equipment and software (Noldus bv, Wageningen, NL, USA).

Supplementary data

Supplementary data are available at *The EMBO Journal* Online (http://www.embojournal.org).

Acknowledgements

We thank M Pilot and O Bernhard for expert technical assistance and W Möbius, head of the EM facility at the MPI for Experimental Medicine, Göttingen. The anti-σ1 serum was a generous gift by M Robinson (Cambridge, UK). All experiments with animals were performed according to the international guidelines. This work was supported by research grants from the Deutsche Forschungsgemeinschaft SFB 523 A6 (to PS) and SFB 523 B10 (to JK).

Conflict of interest

The authors declare that they have no conflict of interest.

References

Aravanis AM, Pyle JL, Tsien RW (2003) Single synaptic vesicles fusing transiently and successively without loss of identity. *Nature* **423:** 643–647

Atluri PP, Ryan TA (2006) The kinetics of synaptic vesicle reacidification at hippocampal nerve terminals. *J Neurosci* **26:** 2313–2320

Balaji J, Armbruster M, Ryan TA (2008) Calcium control of endocytic capacity at a CNS synapse. *J Neurosci* **28:** 6742–6749

Baust T, Czupalla C, Krause E, Bourel-Bonnet L, Hoflack B (2006) Proteomic analysis of adaptor protein 1A coats selectively assembled on liposomes. *Proc Natl Acad Sci USA* **103:** 3159–3164

Bird CM, Burgess N (2008) The hippocampus and memory: insights from spatial processing. *Nat Rev Neurosci* **9:** 182–194

Boehm M, Bonifacino JS (2001) Adaptins: the final recount. *Mol Biol Cell* **12:** 2907–2920

Borner GH, Harbour M, Hester S, Lilley KS, Robinson MS (2006) Comparative proteomics of clathrin-coated vesicles. *J Cell Biol* **175:** 571–578

Ceccarelli B, Hurlbut WP, Mauro A (1973) Turnover of transmitter and synaptic vesicles at the frog neuromuscular junction. *J Cell Biol* **57:** 499–524

Collins BM, McCoy AJ, Kent HM, Evans PR, Owen DJ (2002) Molecular architecture and functional model of the endocytic AP2 complex. *Cell* **109:** 523–535

Cremona O, De Camilli P (1997) Synaptic vesicle endocytosis. *Curr Opin Neurobiol* **7:** 323–330

Doray B, Lee I, Knisely J, Bu G, Kornfeld S (2007) The gamma/sigma1 and alpha/sigma2 hemicomplexes of clathrin adaptors AP-1 and AP-2 harbor the dileucine recognition site. *Mol Biol Cell* **18:** 1887–1896

Fremeau Jr RT, Kam K, Qureshi T, Johnson J, Copenhagen DR, Storm-Mathisen J, Chaudhry FA, Nicoll RA, Edwards RH (2004) Vesicular glutamate transporters 1 and 2 target to functionally distinct synaptic release sites. *Science* **304:** 1815–1819

Gandhi SP, Stevens CF (2003) Three modes of synaptic vesicular recycling revealed by single-vesicle imaging. *Nature* **423:** 607–613

Ghosh P, Dahms NM, Kornfeld S (2003) Mannose 6-phosphate receptors: new twists in the tale. *Nat Rev Mol Cell Biol* **4:** 202–212

Ghosh P, Kornfeld S (2003) AP-1 binding to sorting signals and release from clathrin-coated vesicles is regulated by phosphorylation. *J Cell Biol* **160:** 699–708

Heldwein EE, Macia E, Wang J, Yin HL, Kirchhausen T, Harrison SC (2004) Crystal structure of the clathrin adaptor protein 1 core. *Proc Natl Acad Sci USA* **101:** 14108–14113

Hell SW, Stelzer EH, Lindek S, Cremer C (1994) Confocal microscopy with an increased detection aperture: type-B 4Pi confocal microscopy. *Opt Lett* **19:** 222

Herzog E, Takamori S, Jahn R, Brose N, Wojcik SM (2006) Synaptic and vesicular co-localization of the glutamate transporters VGLUT1 and VGLUT2 in the mouse hippocampus. *J Neurochem* **99:** 1011–1018

Heuser JE, Reese TS (1973) Evidence for recycling of synaptic vesicle membrane during transmitter release at the frog neuromuscular junction. *J Cell Biol* **57:** 315–344

Hüve J, Wesselmann R, Kahms M, Peters R (2008) 4Pi microscopy of the nuclear pore complex. *Biophys J* **95:** 877–885

Janvier K, Kato Y, Boehm M, Rose JR, Martina JA, Kim BY, Venkatesan S, Bonifacino JS (2003) Recognition of dileucine-based sorting signals from HIV-1 Nef and LIMP-II by the AP-1 gamma-sigma1 and AP-3 delta-sigma3 hemicomplexes. *J Cell Biol* **163:** 1281–1290

Jung N, Haucke V (2007) Clathrin-mediated endocytosis at synapses. *Traffic* **8:** 1129–1136

Kantheti P, Qiao X, Diaz ME, Peden AA, Meyer GE, Carskadon SL, Kapfhamer D, Sufalko D, Robinson MS, Noebels JL, Burmeister M (1998) Mutation in AP-3 delta in the mocha mouse links endosomal transport to storage deficiency in platelets, melanosomes, and synaptic vesicles. *Neuron* **21:** 111–122

Kim SH, Ryan TA (2009) Synaptic vesicle recycling at CNS snapses without AP-2. *J Neurosci* **29:** 3865–3874

Lagnado L, Gomis A, Job C (1996) Continuous vesicle cycling in the synaptic terminal of retinal bipolar cells. *Neuron* **17:** 957–967

Matsuda S, Miura E, Matsuda K, Kakegawa W, Kohda K, Watanabe M, Yuzaki M (2008) Accumulation of AMPA receptors in autophagosomes in neuronal axons lacking adaptor protein AP-4. *Neuron* **57:** 730–745

Medigeshi GR, Krikunova M, Radhakrishnan K, Wenzel D, Klingauf J, Schu P (2008) AP-1 membrane-cytoplasm recycling regulated by μ1A-adaptin. *Traffic* **9:** 121–132

Medigeshi GR, Schu P (2003) Characterization of the *in vitro* retrograde transport of MPR46. *Traffic* **4:** 802–811

Meyer C, Eskelinen EL, Guruprasad MR, von Figura K, Schu P (2001) μ1A deficiency induces a profound increase in MPR300/IGF-II receptor internalization rate. *J Cell Sci* **114:** 4469–4476

Meyer C, Zizioli D, Lausmann S, Eskelinen EL, Hamann J, Saftig P, von Figura K, Schu P (2000) μ1A adaptin-deficient mice: lethality, loss of AP-1 binding and rerouting of mannose 6-phosphate receptors. *EMBO J* **19:** 2193–2203

Miesenböck G, De Angelis DA, Rothman JE (1998) Visualizing secretion and synaptic transmission with pH-sensitive green fluorescent proteins. *Nature* **394:** 192–195

Moechars D, Weston MC, Leo S, Callaerts-Vegh Z, Goris I, Daneels G, Buist A, Cik M, van der Spek P, Kass S, Meert T, D'Hooge R, Rosenmund C, Hampson RM (2006) Vesicular glutamate transporter VGLUT2 expression levels control quantal size and neuropathic pain. *J Neurosci* **26:** 12055–12066

Murthy VN, Stevens CF (1998) Synaptic vesicles retain their identity through the endocytic cycle. *Nature* **392:** 497–501

Nakatsu F, Okada M, Mori F, Kumazawa N, Iwasa H, Zhu G, Kasagi Y, Kamiya H, Harada A, Nishimura K, Takeuchi A, Miyazaki T, Watanabe M, Yuasa S, Manabe T, Wakabayashi K, Kaneko S, Saito T, Ohno H (2004) Defective function of GABA-containing synaptic vesicles in mice lacking the AP-3B clathrin adaptor. *J Cell Biol* **167:** 293–302

Newell-Litwa K, Seong E, Burmeister M, Faundez V (2007) Neuronal and non-neuronal functions of the AP-3 sorting machinery. *J Cell Sci* **120:** 531–541

Reusch U, Bernhard O, Koszinowski U, Schu P (2002) AP-1A and AP-3A lysosomal sorting functions. *Traffic* **3:** 752–761

Ricotta D, Hansen J, Preiss C, Teichert D, Höning S (2008) Characterization of a protein phosphatase 2A holoenzyme that dephosphorylates the clathrin adaptors AP-1 and AP-2. *J Biol Chem* **283:** 5510–5517

Robinson MS (2004) Adaptable adaptors for coated vesicles. *Trends Cell Biol* **14:** 167–174

Saint-Pol A, Yelamos B, Amessou M, Mills IG, Dugast M, Tenza D, Schu P, Antony C, McMahon HT, Lamaze C, Johannes L (2004) Clathrin adaptor epsinR is required for retrograde sorting on early endosomal membranes. *Dev Cell* **6:** 525–538

Schmid EM, McMahon HT (2007) Integrating molecular and network biology to decode endocytosis. *Nature* **448:** 883–888

Simmen T, Honing S, Icking A, Tikkanen R, Hunziker W (2002) AP-4 binds basolateral signals and participates in basolateral sorting in epithelial MDCK cells. *Nat Cell Biol* **4:** 154–159

Slepnev VI, De Camilli P (2000) Accessory factors in clathrin-dependent synaptic vesicle endocytosis. *Nat Rev Neurosci* **1:** 161–172

Takamori S, Holt M, Stenius K, Lemke EA, Gronborg M, Riedel D, Urlaub H, Schenck S, Brugger B, Ringler P, Muller SA, Rammner B, Grater F, Hub JS, De Groot BL, Mieskes G, Moriyama Y, Klingauf J, Grubmuller H, Heuser J *et al* (2006) Molecular anatomy of a trafficking organelle. *Cell* **127:** 831–846

Takatsu H, Sakurai M, Shin HW, Murakami K, Nakayama K (1998) Identification and characterization of novel clathrin adaptor-related proteins. *J Biol Chem* **273:** 24693–24700

Takei K, Mundigl O, Daniell L, De Camilli P (1996) The synaptic vesicle cycle: a single vesicle budding step involving clathrin and dynamin. *J Cell Biol* **133:** 1237–1250

Tarpey PS, Stevens C, Teague J, Edkins S, O'Meara S, Avis T, Barthorpe S, Buck G, Butler A, Cole J, Dicks E, Gray K, Halliday K, Harrison R, Hills K, Hinton J, Jones D, Menzies A, Mironenko T, Perry J *et al* (2006) Mutations in the gene encoding the Sigma 2 subunit of the adaptor protein 1 complex, AP1S2, cause X-linked mental retardation. *Am J Hum Genet* **79:** 1119–1124

Voglmaier SM, Kam K, Yang H, Fortin DL, Hua Z, Nicoll RA, Edwards RH (2006) Distinct endocytic pathways control the rate and extent of synaptic vesicle protein recycling. *Neuron* **51:** 71–84

Wang YJ, Wang J, Sun HQ, Martinez M, Sun YX, Macia E, Kirchhausen T, Albanesi JP, Roth MG, Yin HL (2003) Phosphatidylinositol 4 phosphate regulates targeting of clathrin adaptor AP-1 complexes to the Golgi. *Cell* **114:** 299–310

Wenk MR, De Camilli P (2004) Protein–lipid interactions and phosphoinositide metabolism in membrane traffic: insights from vesicle recycling in nerve terminals. *Proc Natl Acad Sci USA* **101:** 8262–8269

Wienisch M, Klingauf J (2006) Vesicular proteins exocytosed and subsequently retrieved by compensatory endocytosis are non-identical. *Nat Neurosci* **9:** 1019–1027

Wojcik SM, Rhee JS, Herzog E, Sigler A, Jahn R, Takamori S, Brose N, Rosenmund C (2004) An essential role for vesicular glutamate transporter 1 (VGLUT1) in postnatal development and control of quantal size. *Proc Natl Acad Sci USA* **101:** 7158–7163

Wu LG, Ryan TA, Lagnado L (2007) Modes of vesicle retrieval at ribbon synapses, calyx-type synapses, and small central synapses. *J Neurosci* **27:** 11793–11802

Wucherpfennig T, Wilsch-Brauninger M, Gonzalez-Gaitan M (2003) Role of *Drosophila* Rab5 during endosomal trafficking at the synapse and evoked neurotransmitter release. *J Cell Biol* **161:** 609–624

Zizioli D, Meyer C, Guhde G, Saftig P, von Figura K, Schu P (1999) Early embryonic death of mice deficient in γ-adaptin. *J Biol Chem* **274:** 5385–5390

